



Origin of ferroelastic domains in free-standing single-crystal ferroelectric films

I. A. Luk'yanchuk

Laboratory of Condensed Matter Physics, University of Picardie Jules Verne, Amiens 80039, France
and L. D. Landau Institute for Theoretical Physics, Moscow, Russia

A. Schilling and J. M. Gregg

Centre for Nanostructured Media, School of Maths and Physics, Queen's University of Belfast, University Road, Belfast BT7 1NN, United Kingdom

G. Catalan and J. F. Scott

Department of Earth Sciences, University of Cambridge, Downing Street, Cambridge CB2 3EQ, United Kingdom
(Received 29 January 2009; revised manuscript received 4 March 2009; published 8 April 2009)

The origin of the unusual 90° ferroelectric/ferroelastic domains, consistently observed in recent studies on mesoscale and nanoscale free-standing single crystals of BaTiO_3 [Schilling *et al.*, Phys. Rev. B **74**, 024115 (2006); Schilling *et al.*, Nano Lett. **7**, 3787 (2007)], has been considered. A model has been developed which postulates that the domains form as a response to elastic stress induced by a surface layer which does not undergo the paraelectric-ferroelectric cubic-tetragonal phase transition. This model was found to accurately account for the changes in domain periodicity as a function of size that had been observed experimentally. The physical origin of the surface layer might readily be associated with patterning damage, seen in experiment; however, when all evidence of physical damage is removed from the BaTiO_3 surfaces by thermal annealing, the domain configuration remains practically unchanged. This suggests a more intrinsic origin, such as the increased importance of surface tension at small dimensions. The effect of surface tension is also shown to be proportional to the difference in hardness between the surface and the interior of the ferroelectric. The present model for surface-tension induced twinning should also be relevant for finely grained or core-shell structured ceramics.

DOI: [10.1103/PhysRevB.79.144111](https://doi.org/10.1103/PhysRevB.79.144111)

PACS number(s): 77.80.Bh, 77.55.+f, 77.80.Dj

I. INTRODUCTION

In 1935 Landau and Lifshitz¹ predicted the appearance of periodic thermodynamically stable domains, with oppositely oriented magnetic moments, in ferromagnetic crystals. The existence of these domains minimized the energy of the depolarizing field caused by the abrupt discontinuity of the spontaneous magnetization at the sample surface. Additional consideration of the associated domain-wall energies allowed them to predict a square-root dependence of the domain period on the sample thickness. This square-root relationship is often referred to as the Kittel law because of its independent formulation in 1946 by Kittel.² The law is also valid for 180° domains in ferroelectric crystals,^{3,4} where the unfavorable depolarizing electric field is provided by the abrupt polar discontinuity at the surface. The Landau-Lifshitz-Kittel theory was later extended by Roitburd⁵ to describe the behavior of ferroelastic domains formed as a result of substrate clamping effects in thin-film systems.

In previous studies we have shown that the Kittel law works perfectly for a wide class of ferroic materials (ferromagnetic, ferroelectric, or ferroelastic) over six orders of magnitude in film thickness,^{6,7} and that it can be intuitively expressed in terms of the domain-wall thickness.⁸⁻¹⁰ Moreover, we have demonstrated that the Kittel approach can be extended to three-dimensional structures,¹¹⁻¹³ to ferroelectric superlattices,⁹ and to multiferroic materials.^{14,15} Much of the experimental work has been in association with observations of periodic 90° ferroelectric-ferroelastic domains that have

been consistently observed in free-standing single-crystal thin films [see Fig. 1(a)] and nanowires of BaTiO_3 . In all our experiments, the size of the 90° domains as a function of size is indeed found to be well described by a Kittel-Roytburd formalism.

At first glance, however, the very existence of such domains in our free-standing samples is quite surprising. Ferroelastic domains normally appear in response to an external stress (such as that imposed by clamping to a rigid substrate, for example) which forces the sample toward shape preservation in the clamped directions. The domain configuration is such that the macroscopic shape difference between the paraphase and the ferrophase is minimized while the domain size responds to an equilibrium between domain energy and

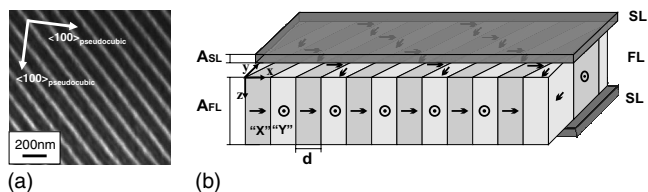


FIG. 1. (a) Scanning transmission electron microscopy image of periodic domain structure in free-standing single-crystal lamella of BaTiO_3 . (b) Sketch of our model system, comprising a FL sandwiched between two SL which do not undergo the ferroelastic transformation. The stress imposed by these untransformed “dead” layers onto the ferroelectric layer induces the appearance of 90° ferroelectric/ferroelastic domains

domain-wall energy.⁵ However, our BaTiO₃ lamella are free-standing single crystals and therefore free from epitaxially induced stress, so they have no Roytburd-type interface-induced elastic driving force. The question, then, is the following: if there is no external stress, what causes the appearance of the ferroelastic domains?

In the present work we explain the appearance of the self-organized domain patterns in free-standing nanosamples of BaTiO₃ by assuming that the driving stress is provided by an encapsulating surface layer. In much of our experimental work, this encapsulation layer could easily be associated with the surface damage caused by focused ion-beam (FIB) milling. However, we have also observed here that 90° domains persist, with only slightly altered periodicities, even when surface damage has been repaired by thermal annealing; this suggests that the strain effects may in fact arise intrinsically from surface tension, being therefore unavoidable even in nominally “perfect” free-standing ferroelectric nanostructures.

II. MODEL

The development of the model focuses on the geometry of the single-crystal lamellas first reported in Ref. 7, an example of which is shown in Fig. 1(a). Figure 1(b) shows a schematic cross section of our model representation for such BaTiO₃ lamella, with the surface encapsulation layers (SLs) that are potentially responsible for the formation of 90° domains present and their obedience to Kittel behavior. The model comprises a tetragonal ferroelectric/ferroelastic layer (FL) of thickness A_{FL} , exemplified by BaTiO₃, sandwiched between two cubic paraelectric SL of thickness A_{SL} . The surface layers provide the stress for the creation of the ferroelectric-ferroelastic domains in the FL. The assumption of cubic surfaces is supported by the observation that barium titanate nanoparticles have a core-shell structure with tetragonal interior and cubic surfaces.^{16,17} However, the cubic symmetry is not a key feature of the model: for the SL to impose stress on the interior, it is just sufficient that it does not undergo the phase transition at T_C . A nonferroelectric capsule/matrix was also assumed in recent phase-field simulations of domain patterns in ferroelectric nanostructures.¹⁸

In the present model, the SL thickness is an adjustable parameter to be determined from experimental measurements. The Cartesian z axis is oriented perpendicular to the plane of the lamella, and the x and y axes coincide with the crystal axes of BaTiO₃ as shown in Fig. 1(a). The equilibrium lattice parameters of the FL are assumed to be those of the bulk ferroelectric tetragonal BaTiO₃ crystal and, in order to minimize depolarization fields, the polarization will tend to lie within the XY plane, pointing parallel to either the X or Y directions. In terms of notation, $[c_0, a_0, a_0]$ if P is parallel to x or $[a_0, c_0, a_0]$ if P is parallel to y . The formation of the SL with different equilibrium lattice constants $[b_0, b_0, b_0]$ results in elastic stress, provided by lattice matching at the FL and SL interface.

Consider starting with the simplest possibility when the matching stress is uniform, i.e., there are no stress gradients. Because the SL is much thinner than the FL, the latter re-

mains undeformed, keeping the equilibrium BaTiO₃ lattice parameters ($[c_0, a_0, a_0]$ or $[a_0, c_0, a_0]$). Deformation concerns only the SL which, because of the matching conditions, should conserve the same XY -plane parameters as the FL but can relax in the Z direction ($s_{zz}=0$). The corresponding deformation energy is caused by the in-plane misfit strains of SL, and contains the tension and shear parts.^{19–22}

$$W_{\text{SL}} = 2 \frac{GA_{\text{SL}}}{1-\nu} (s_a'^2 + 2\nu s_a' s_c' + s_c'^2) \\ = A_{\text{SL}} G \frac{1+\nu}{1-\nu} (\delta_{ab} + \delta_{cb})^2 + A_{\text{SL}} G \delta_{ca}^2, \quad (1)$$

where the diagonal components of the plain strain tensor of SL $(s_a', s_c', 0) = (s'_{xx}, s'_{yy}, s'_{zz})$ are expressed via the mismatch parameters:

$$s_a' = \delta_{ab} = \frac{a_0 - b_0}{b_0}, \quad s_c' = \delta_{cb} = \frac{c_0 - b_0}{b_0}, \\ s_a' - s_c' = \delta_{ca} = \frac{c_0 - a_0}{b_0}, \quad (2)$$

G is the shear modulus, ν is the Poisson ratio, and the factor of 2 corresponds to two (top and bottom) SLs on both sides of the FL. We assume that $G \approx 40 \times 10^9 - 55 \times 10^9$ N m⁻² (Ref. 23) and $\nu \approx 0.28$ (Ref. 24) are approximately the same for SL and FL.

Such system can be unstable toward formation of the experimentally observed periodic structure of 90° ferroelastic domains $X/Y/X/Y$ shown in Fig. 1. Usually, such domains have 45° domain walls and “head-to-tail” polarization contacts to avoid the formation of depolarization charge. The reason of the instability is that domain formation can reduce the elastic energy (1) of the SL by allowing the misfit stress to gradually relax inside the FL within an interfacial region whose thickness is of the order of the domain width d . The domains will appear when the elastic energy imposed onto the SL by the ferroelectric is bigger than the energy required for the formation of domain walls. We emphasize that, although the net effect of ferroelastic twinning is to minimize the macroscopic deformation of the SL, this twinning necessarily requires a strain gradient near the interface. This is because, while far away from the interface the lattice parameters of the FL are those of the bulk ferroelectric, at the interface they must become closer to cubic in order to match the SL. Accordingly, an inhomogeneously strained region must appear for which flexoelectric effects may be important.^{25–28} The flexoelectric contribution, however, has been left out of this model for the sake of simplicity.

The situation described here is in fact quite similar to the appearance of periodic 90° domains in epitaxial ferroelectric films strained by thick undeformable substrates^{19,20,22} in which the film/substrate mismatch strain relaxes in the near-surface layer of the film. The only difference is that the contact elastic SL in our case is thin and its deformation should be considered self-consistently with that of FL. In a way, the

model discussed here can be seen as a generalization of the substrate/film models for the case of a substrate that has finite thickness compared with the film.

The mechanism of nonuniform strain relaxation in the domain-populated FL gives rise to two new energy contributions: the near-surface deformation energy of the ferroelectric layer, W_{FL} , and the energy of the domain walls W_{DW} . The energy balance between W_{SL} , W_{FL} , and W_{DW} optimizes the domain period $2d$, and the matching plane lattice constants changing periodically at the SL/FL interface from (c, a) at the X domain to (a, c) at the Y domain.

Before proceeding to the derivation of the total energy of the system

$$W = 2W_{FL} + 2W_{SL} + W_{DW} \quad (3)$$

(the factors of 2 correspond to two-side SL and two-side relaxation near-surface layers in FL), we assume that the optimal domain width d is thinner than the FL but thicker than the SL:

$$A_{SL} < d < A_{FL}. \quad (4)$$

Observed in experiment and discussed in detail later, such hierarchy simplifies the calculation of the different contributions to Eq. (3).

We express the deformation energy W_{FL} of the ferroelectric layer in terms of periodically changing strains of domains $(s_a, s_c)/(s_c, s_a)$ at the surface of the FL,

$$s_c = \frac{c - c_0}{c_0}, \quad s_a = \frac{a - a_0}{a_0}. \quad (5)$$

These are taken as variational parameters in the general expression for the elastic energy of the two-dimensional crystal, periodically strained as $(s_a, s_c)/(s_c, s_a)$ and with relative domain population equal to ϕ [see also Eq. (30) in Ref. 22]:

$$W_{FL} = \frac{GA_{FL}}{1-\nu}(s_a^2 + 2\nu s_a s_c + s_c^2) + GA_{FL}(s_a - s_c)^2 \times \left[-2\phi + \frac{2d}{A_{FL}} f_a \left(\frac{2d}{A_{FL}}, \phi \right) \right]. \quad (6)$$

Adapting Eq. (6) to the case of equally populated ($\phi = 1/2$) and thin ($d < A_{FL}$) domains, the universal dimensionless function can be simplified as: $f_a \approx A_{FL}/4d + 7\zeta(3)/8\pi^3$,²² and therefore:

$$W_{FL} = \frac{1}{2}A_{FL}G \frac{1+\nu}{1-\nu} (s_a + s_c)^2 + \frac{1}{2}\kappa^{-1}dG(s_a - s_c)^2, \quad (7)$$

$$\kappa = \frac{2\pi^3}{7\zeta(3)} \approx 7.4.$$

Physically, the first term in Eq. (7) corresponds to the average interface-induced strain that propagates through the whole thickness A_{FL} of the FL. The second term is produced by the superposition of alternative strains of an infinite series of domains, compensating inside the FL and relaxing in the near-surface gradient layer of a thickness of order d . Technically this sum is expressed via the zeta function $\zeta(3)$, like the

electrostatic energy of alternative depolarization charge compensation in Kittel formula for ferroelectric domains.^{1,2}

Before minimizing Eq. (7) we can ensure first the vanishing of the largest first (volume) term, selecting $s_a + s_c = 0$; this is justified because the domain pattern can compensate for shear strains $(s_a - s_c)$ but not for volume changes. The number of variational parameters then reduces to one: $s \equiv s_a = -s_c$ and the second (surface) term takes the form:

$$W_{FL} = 2\kappa^{-1}dGs^2. \quad (8)$$

Consider now the deformation energy W_{SL} of the SL subjected to $2d$ -periodic domain-induced surface strains $(s'_a, s'_c)/(s'_c, s'_a)$, taking into account that s'_a and s'_c are expressed via variational parameters s_a and s_c [Eq. (5)] as

$$s'_c = \frac{c - b_0}{b_0} \approx s_c + \delta_{cb}, \quad s'_a = \frac{a - b_0}{b_0} \approx s_a + \delta_{ab}. \quad (9)$$

If the SL is thinner than the domain structure period ($A_{SL} \ll d$), the periodic surface strain does not manage to relax across the SL. Then, SL can be presented as a piecewise $(s'_a, s'_c)/(s'_c, s'_a)$ strained film, having uniform deformation for each section. Summing the given by the first part of Eq. (1) elastic energies from all the pieces (that are equal because of the $s'_a \leftrightarrow s'_c$ symmetry) and taking into account the discussed above constrain $s_a = -s_c = s$, we present the elastic energy of the SL as a superposition of tension and shear contributions:

$$W_{SL} = \frac{1}{2}A_{SL}G \frac{1+\nu}{1-\nu} (\delta_{ab} + \delta_{cb})^2 + \frac{1}{2}A_{SL}G(2s - \delta_{ac})^2. \quad (10)$$

Note that the tension contribution:

$$W_T = \frac{1}{2}A_{SL}G \frac{1+\nu}{1-\nu} (\delta_{ab} + \delta_{cb})^2, \quad (11)$$

does not depend on strain variational parameter s and coincides with the tension energy of the uniformly deformed SL in Eq. (1).

Combining Eqs. (8) and (10) with the energy of domain walls

$$W_{DW} = \sigma \frac{A_{FL}}{d} \quad (12)$$

(σ is the surface energy density of the domain walls), the total energy (3) is

$$W = W_T + \sigma \frac{A_{FL}}{d_0} \left[\frac{d}{d_0} r^2 + \kappa \frac{A_{SL}}{d_0} (r-1)^2 + \frac{d_0}{d} \right], \quad (13)$$

where $r = 2s / \delta_{ca}$ and

$$d_0 = \sqrt{\kappa D A_{FL}} = 2.7 \sqrt{D A_{FL}}, \quad (14)$$

with the length-scale parameter

$$D = \frac{\sigma}{G \delta_{ca}^2} \approx 0.5 \text{ nm}, \quad (15)$$

which can be interpreted as ‘‘domain-wall half thickness.’’ This value is ca. one-two lattice constants, and agrees with

previously reported theoretical and experimental values.^{29–32}

Minimization of Eq. (13) over r and d gives the expression for optimal domain width

$$d = \frac{d_0}{1 - \frac{d_0}{\kappa A_{SL}}}. \quad (16)$$

When $d_0 \ll \kappa A_{SL}$, one can neglect the term in the denominator responsible for the upward curvature in Eq. (16) and obtain the Kittel-type dependence [Eq. (14)] for $d(A_{FL})$. This explains why our experimental results could be reasonably well fitted assuming a simple square-root dependence of domain periodicity on film thickness.⁷ Note however that we are still in the thin surface layer limit $A_{SL} < d_0$. The opposite (irrelevant for our system) limit $d_0 < \kappa A_{SL}$ will lead to the Roytburd-Pompe-Pertsev situation of thick substrate with domain pattern also obeying the Kittel law but with a different numerical constant. When $d_0 \rightarrow \kappa A_{SL}$, the domain width diverges, implying a transition to a monodomain state. Domains therefore exist only when

$$d_0 < \kappa A_{SL}, \quad (17)$$

or, taking into account Eqs. (14) and (16), when

$$A_{FL} \lesssim 7.4 \frac{A_{SL}^2}{D}, \quad (18)$$

where D is estimated as Eq. (15). This represents a rather narrow constraint, providing assumption (4) is satisfied.

Substitution of the optimal parameters r and d into Eq. (13) gives the energy of the domain state

$$W = W_T + 2 \frac{d_0}{\kappa A_{SL}} \left[1 - \frac{1}{2} \frac{d_0}{\kappa A_{SL}} \right] A_{SL} \delta_{ac}^2 G, \quad (19)$$

which is smaller than Eq. (1) [since $2x(1-x/2) \leq 1$ with $x = d_0/\kappa A_{SL}$] in the limits of applicability of the theory. This confirms the instability of the ferroelectric free-standing lamella with surface tension toward domain formation.

III. COMPARISON WITH EXPERIMENT

An attempt was made to use the model developed above to describe the variation in domain periodicity observed for single-crystal BaTiO₃ lamellas quantitatively. To do this it was noted that the previously published domain period data⁷ had all been taken from lamellas for which there had been no attempt to repair surface damage caused by FIB processing. It was expected that physical “encapsulation layers” of amorphous BaTiO₃ should exist on the top and bottom lamellar surfaces. To establish the thickness of the physically damaged layers, cross-sectional transmission electron microscopy (TEM) was used, with the lamellar cross sections prepared by FIB according to the schematic shown in Fig. 2. As can be seen in Fig. 3, a surface layer of amorphous material, approximately 20 nm in thickness, was indeed observed. In conjunction with energy dispersive x-ray data, this layer was categorized as a gallium-impregnated barium titanate glass.

Substitution of this glassy layer thickness as that of an encapsulation layer (A_{SL}) and using a domain-wall energy

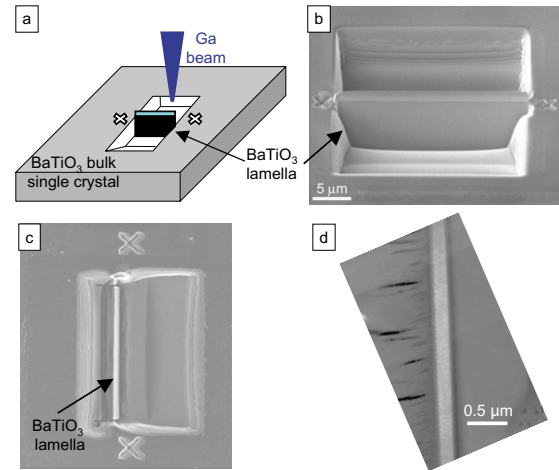


FIG. 2. (Color online) Different stages of a FIB process to fabricate a BaTiO₃ lamella for cross-sectional view: (a) schematic drawing of a lamella milled by FIB. Prior to milling, a protective rim of either Au or Pt (strip in the top edge of the lamella in the sketch) was deposited in order to help minimize Ga damage during milling, (b) FIB image of a lamella tilted at 45° for better viewing, (c) vertical view, and (d) cross-sectional TEM image of a lamella milled by FIB.

density of $\sigma = 3 \times 10^{-3} \text{ J m}^{-1}$ (Ref. 29) produced a remarkably good quantitative description of the observed domain periodicity data, as can be seen in Fig. 4. This strong agreement was obtained without any free fitting parameters, and one might naturally conclude that all of the encapsulation suffered by the BaTiO₃ lamellas was indeed due to the constraint from the ion-beam damaged layers.

However, we have spent some considerable effort to develop processing methodologies to repair the surface damage caused by focused ion-beam processing. Thermal annealing in air at 700 °C has been seen to both recrystallize the damage and expel the implanted gallium (forming thin gallium oxide platelets), recovering pristine single-crystal BaTiO₃ (Refs. 33–35) (see Fig. 5). If the thermal annealing is performed in oxygen, then functional measurements even suggest that the permittivity of the surface region is the same as that seen in bulk.^{33,35}

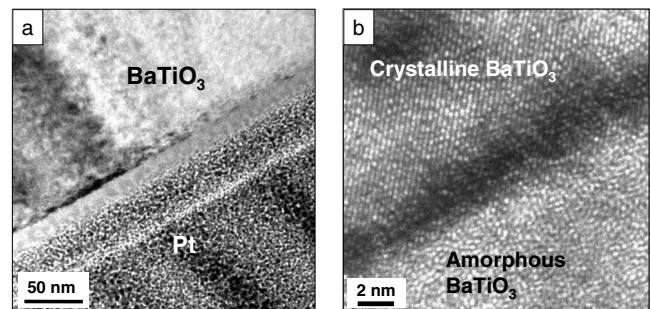


FIG. 3. (a) High-resolution transmission electron microscopy (HRTEM) image of a cross-sectional BaTiO₃ lamella after FIB milling showing a 20-nm-thick damaged layer at the Pt/BaTiO₃ interface (the Pt epilayer was deposited to preserve the original surface structure associated with FIB processing of the lamellas). (b) Zoom in on the damage layer, showing its amorphous structure.

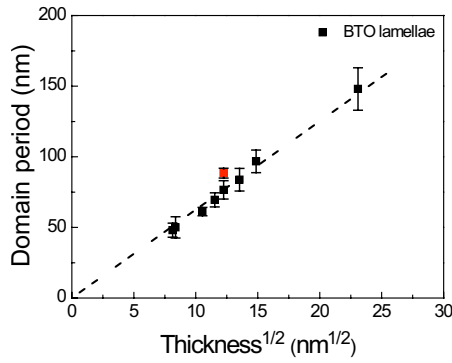


FIG. 4. (Color online) Solid data in black color: experimentally measured domain period as a function of thickness for free-standing single-crystal films of ferroelectric BaTiO_3 with a surface layer thickness of ~ 20 nm. The red color point represents the domain period after annealing at 700°C for 1 h in air. For a lamella thickness of 150 nm, the domain period changes from 76.6 ± 6.5 nm (before annealing) to 88.4 ± 3.5 nm (after annealing). Dotted line, calculation using Eq. (16) assuming $A_{\text{SL}} = 20$ nm, and a domain-wall energy density of $\sigma \approx 3 \times 10^{-3} \text{ J m}^{-1}$ (Ref. 29). The agreement is good without free fitting parameters

The domain structure seen in a lamella which had been thermally annealed and is expected to have no surface damage is shown in Fig. 5(c). The domain appearance is almost identical to the unannealed sample in Fig. 1, with the domain walls still of $\{110\}$ type, indicating that 90° domain sets have again formed. While gallium oxide platelets have precipitated on the annealed surface [the white blotches in Fig. 5(c)], these platelets certainly do not form a continuous layer, and it seems unlikely that they can provide the homogeneous stress needed to induce the 90° domain sets observed. Further, when the periodicity of the domains is analyzed and compared to that obtained in unannealed lamellas, only a slight increase in domain period is observed; the increase in domain period is in fact consistent with an effective increase in the thickness of the lamella by 40 nm (that associated with the recrystallization of the amorphous glassy regions described above). The essential physics at play therefore appears to be unchanged even when the extrinsic damage layer is removed.

Overall, then, it appears that the quantitative agreement between the model and our data may be fortuitous, and that

the stress responsible for the domains is not necessarily coming from the glassy barium titanate. Instead, a more fundamental source of stress must be at play for all of the FIBed single-crystal barium titanate lamellas investigated to date. This suggests the existence of an intrinsic surface relaxation layer, probably due to surface tension.

The existence of surface layers in BaTiO_3 has been known for quite some time,^{16,17,36–43} yet there is surprisingly little agreement about their properties. Experimentally, their thickness seems to be on the region of 5–10 nm or more,^{16,17,36–38} whereas first-principles calculations give a much smaller value, about 1 nm.^{39–42} In some works the SL is found to be tetragonal at all temperatures, even above T_C ,^{36,37} where in others it is cubic even below T_C .^{16,17} In fact, the structure of the SL can be rather complex and depends on processing conditions.⁴³ Nevertheless, what is important from the point of view of our model is not so much the exact symmetry of the surface but the fact that it does not undergo the same ferroelectric/ferroelastic phase transition as the inside of the film. Thus, when the film becomes ferroelectric, it automatically becomes stressed by the untransformed surface layer. The present model requires only that the induced stress is isotropic or orthotropic, and this is the case not only with cubic SLs but also with either amorphous SL or with tetragonal SL provided that the tetragonal axis is out of plane.

On the other hand, the elastic energy stored by the surface layer is proportional to its thickness. The outstanding question, then, is whether an intrinsic and very thin SL due to surface tension can lead to the same domain size as would be expected from the thicker encapsulation layers seen in our unannealed samples.

Indeed, Eq. (16) states that the domain size is essentially d_0 , independent of the SL thickness; however, this equation is only valid when $d_0 \ll \kappa A_{\text{SL}}$, which is not true if $A_{\text{SL}} \approx 1$ nm. On the other hand, our model has implicitly assumed that the stiffness (the shear modulus G) is the same for FL and SL, and this is unlikely when the SL is an intrinsic surface-tension layer; for these, the bonds are known to be shorter⁴² and the SL should be expected to be harder than the FL. It is relatively straightforward to incorporate the different shear modulus of the surface layer (G_{SL}) and the ferroelectric layer (G_{FL}) onto the model by simply substituting G for G_{FL} and G_{SL} in Eqs. (8) and (10), respectively. Minimi-

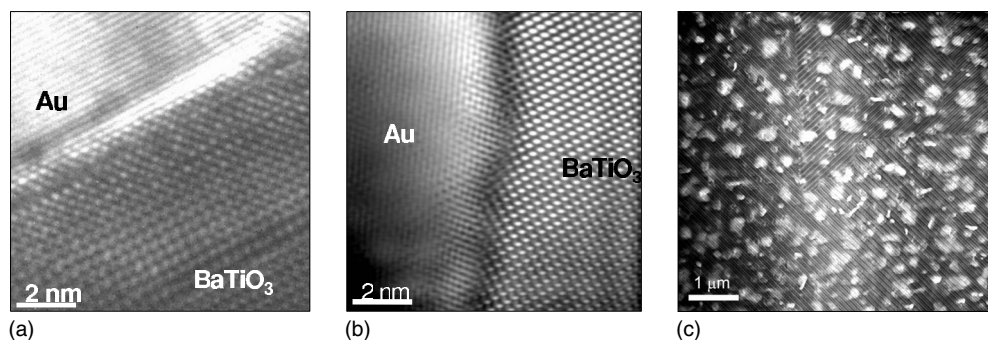


FIG. 5. (a) HRTEM image of a cross-sectional BaTiO_3 lamella after FIB milling and annealing at 700°C in air. (b) An inverse FFT image of the Au/ BaTiO_3 interface showing the complete reconstructed structure by postannealing. Lattice fringes are evident up to the boundary with an Au protective layer, with no evidence of amorphization. (c) Plain-view TEM image of the annealed lamella, showing the expelled Ga as clusters on the surface and the persistence of the regular domain pattern.

zation of the total energy then leads to the generalized expression for domain size:

$$d = \frac{d_0}{1 - \frac{d_0}{\kappa A_{SL}} \frac{G_{FL}}{G_{SL}}}. \quad (20)$$

This expression is almost identical to Eq. (16) except for the appearance of the factor G_{FL}/G_{SL} in the denominator. This factor can compensate for a reduced thickness of the surface layer insofar as its hardness is greater than that of the ferroelectric layer. Presently we have no quantitative estimates for the hardness of the intrinsic epilayer, and we very much encourage the theoretical community to perform first-principles calculations of the value of G_{SL} . What we can say is that, if the thickness of the SL is only 1–2 nm, as suggested by the *ab initio* calculations,^{39–42} its shear modulus would need to be roughly ten times bigger than that of the FL to have the same effect on domain size as our 20 nm extrinsic encapsulation layer. If, however, the true thickness of the intrinsic SL is ca. 10 nm, as suggested by experimental measurements,^{16,17,36–38} then the SL need not be any more rigid than the FL.

IV. CONCLUSIONS

In sum, we have shown that, even in the absence of rigid substrates or any other source of external stress, ferroelastic twinning can appear due to the self-stress imposed by surface layers. The importance of such layers obviously increases as the size of the system decreases such that this effect becomes particularly important at the nanoscale. Furthermore, there need not be an extrinsic surface layer for the ferroelastic domains to appear; surface tension, which is intrinsic and therefore unavoidable, can also provide the necessary stress for domain formation. Finally, we note that epilayers can be expected to be important not only for isolated nanoferroelectrics but also in macroscopic devices such as ceramic capacitors made with nanopowders or core-shell grains.

ACKNOWLEDGMENTS

This work was supported by the EC Project No. FP6-STREP-MULTICERAL and by the French-U.K. collaboration program “Alliance.”

-
- ¹L. D. Landau and E. M. Lifshitz, *Phys. Z. Sowjetunion* **8**, 153 (1935).
²C. Kittel, *Phys. Rev.* **70**, 965 (1946).
³T. Mitsui and J. Furuichi, *Phys. Rev.* **90**, 193 (1953).
⁴S. K. Streiffer, J. A. Eastman, D. D. Fong, C. Thompson, A. Munkholm, M. V. Ramana Murty, O. Auciello, G. R. Bai, and G. B. Stephenson, *Phys. Rev. Lett.* **89**, 067601 (2002).
⁵A. L. Roitburd, *Phys. Status Solidi A* **37**, 329 (1976).
⁶J. F. Scott, *J. Phys.: Condens. Matter* **18**, R361 (2006).
⁷A. Schilling, T. B. Adams, R. M. Bowman, J. M. Gregg, G. Catalan, and J. F. Scott, *Phys. Rev. B* **74**, 024115 (2006).
⁸G. Catalan, J. F. Scott, A. Schilling, and J. M. Gregg, *J. Phys.: Condens. Matter* **19**, 022201 (2007).
⁹V. A. Stephanovich, I. A. Luk'yanchuk, and M. G. Karkut, *Phys. Rev. Lett.* **94**, 047601 (2005).
¹⁰F. De Guerville, I. Luk'yanchuk, L. Lahoche, and M. El Marssi, *Mater. Sci. Eng., B* **120**, 16 (2005).
¹¹A. Schilling, R. M. Bowman, J. M. Gregg, G. Catalan, and J. F. Scott, *Appl. Phys. Lett.* **89**, 212902 (2006).
¹²G. Catalan, A. Schilling, J. F. Scott, and J. M. Gregg, *J. Phys.: Condens. Matter* **19**, 132201 (2007).
¹³A. Schilling, R. M. Bowman, G. Catalan, J. F. Scott, and J. M. Gregg, *Nano Lett.* **7**, 3787 (2007).
¹⁴G. Catalan, H. Bea, S. Fusil, M. Bibes, P. Paruch, A. Barthelemy, and J. F. Scott, *Phys. Rev. Lett.* **100**, 027602 (2008).
¹⁵M. Daraktchiev, G. Catalan, and J. F. Scott, *Ferroelectrics* **375**, 122 (2008).
¹⁶T. Takeuchi, K. Ado, T. Asai, H. Kageyama, Y. Saito, C. Masquelier, and O. Nakamura, *J. Am. Ceram. Soc.* **77**, 1665 (1994).
¹⁷M. Tanaka and Y. Makino, *Ferroelectr., Lett. Sect.* **24**, 13 (1998).
¹⁸J. Slutsker, A. Artemev, and A. Roytburd, *Phys. Rev. Lett.* **100**, 087602 (2008).
¹⁹W. Pompe, X. Gong, Z. Suo, and J. S. Speck, *J. Appl. Phys.* **74**, 6012 (1993).
²⁰J. S. Speck and W. Pompe, *J. Appl. Phys.* **76**, 466 (1994).
²¹J. S. Speck, A. C. Datkin, A. Siefert, A. E. Romanov, and W. Pompe, *J. Appl. Phys.* **78**, 1696 (1995).
²²N. A. Pertsev and A. G. Zembilgotov, *J. Appl. Phys.* **78**, 6170 (1995).
²³B. L. Cheng, M. Gabbay, and G. Fantozzi, *J. Mater. Sci.* **31**, 4141 (1996).
²⁴G. Bradfield, *Nuovo Cimento* **7**, 182 (1950).
²⁵W. Ma and L. E. Cross, *Appl. Phys. Lett.* **88**, 232902 (2006).
²⁶G. Catalan, L. J. Sinnamon, and J. M. Gregg, *J. Phys.: Condens. Matter* **16**, 2253 (2004).
²⁷G. Catalan, B. Noheda, J. McAneney, L. J. Sinnamon, and J. M. Gregg, *Phys. Rev. B* **72**, 020102(R) (2005).
²⁸M. S. Majdoub, R. Maranganti, and P. Sharma, *Phys. Rev. B* **79**, 115412 (2009).
²⁹V. A. Zhirnov, *Sov. Phys. JETP* **35**, 822 (1959).
³⁰B. Meyer and D. Vanderbilt, *Phys. Rev. B* **65**, 104111 (2002).
³¹N. Floquet and C. Valot, *Ferroelectrics* **234**, 107 (1999).
³²D. Shilo, G. Ravichandran, and K. Bhattacharya, *Nature Mater.* **3**, 453 (2004).
³³M. M. Saad, R. M. Bowman, and J. M. Gregg, *Appl. Phys. Lett.* **84**, 1159 (2004).
³⁴A. Schilling, T. Adams, R. M. Bowman, and J. M. Gregg, *Nanotechnology* **18**, 035301 (2007).
³⁵L. W. Chang, M. McMillen, F. D. Morrison, J. F. Scott, and J. M. Gregg, *Appl. Phys. Lett.* **93**, 132904 (2008).
³⁶M. Anliker, H. R. Brugger, and W. Kanzig, *Helv. Phys. Acta* **27**, 99 (1954).
³⁷W. Kanzig, *Phys. Rev.* **98**, 549 (1955).

³⁸Feng Tsai and J. M. Cowley, *Appl. Phys. Lett.* **65**, 1906 (1994).

³⁹J. Padilla and D. Vanderbilt, *Phys. Rev. B* **56**, 1625 (1997).

⁴⁰B. Meyer, J. Padilla, and D. Vanderbilt, *Faraday Discuss.* **114**, 395 (1999).

⁴¹C. Bungaro and K. M. Rabe, *Phys. Rev. B* **71**, 035420 (2005).

⁴²R. I. Eglitis and D. Vanderbilt, *Phys. Rev. B* **76**, 155439 (2007).

⁴³A. M. Kolpak, D. Li, R. Shao, A. M. Rappe, and D. A. Bonnell, *Phys. Rev. Lett.* **101**, 036102 (2008).